Finetuning of the redoxfunction of Pseudomonasaeruginosacytochromec551 through structuralproperties of apolypeptideloopbearing an axialMetresidue

doi: 10.1016/j.jinorgbio.2011.11.027

Fine tuning of the redox function of *Pseudomonas aeruginosa* cytochrome c_{551} through structural properties of a polypeptide loop bearing an axial Met residue

Hulin Tai, Tsuyoshi Udagawa, Shin-ichi Mikami, Akihiro Sugimoto, and Yasuhiko Yamamoto*
Department of Chemistry, University of Tsukuba, Tsukuba 305-8571, Japan

Highlights

The redox function of *P. aeruginosa* cytochrome *c*. is finely tuned by the Ser52 residue. The structure of the loop near the heme is slightly altered by the S52G mutation. The structural change of the loop increases the polarity of the heme environment. As a result, the redox function of the protein is affected by the mutation. Thus, the protein function can be tuned through the structure of the loop.

Corresponding author: E-mail address: yamamoto@chem.tsukuba.ac.jp

Abstract

Pseudomonas aeruginosa cytochrome c_{551} (PA) possesses a long polypeptide loop near its heme, and a unique hydrogen bond network among Ser52, axial Met61, and the heme 13-propionate side chain, i.e., Ser52 amide NH is hydrogen bonded to axial Met61 carbonyl CO, Met61 amide NH to Ser52 carbonyl CO, and Ser52 side chain OH to the heme 13-propionate side chain, contributes to stabilization of the structure of the loop [Y. Matsuura, T. Takano, R.E. Dickerson, J. Mol. Biol. 156 (1982) 389-409]. In this study, the structure and redox function of S52N and S52G mutants were characterized in order to elucidate the role of Ser52 in functional regulation of the protein. We found that the redox function of PA was hardly affected by an S52N mutation, but was slightly by an S52G one. The functional similarity between the wild-type protein and the S52N mutant demonstrated that Asn52 in the mutant plays a similar pivotal role in the formation of the unique hydrogen bond network that stabilizes the structure of the loop as Ser52 in the wild-type protein does. On the other hand, the functional alteration induced by the S52G mutation can be attributed to a structural change of the loop due to the lack of the hydrogen bond between the Gly52 and heme 13-propionate side chain in the mutant. Thus, this study demonstrated that the function of the protein can be tuned through the structural properties of the polypeptide loop near its heme.

Keywords

Cytochrome *c*, Heme, Hydrogen bond, NMR, Protein stability, Redox potential

1. Introduction

Cytochrome *c* (cyt *c*), in which the heme Fe is coordinated to a His and a Met as axial ligands at the redox center, is one of the best-characterized redox proteins, much having been learned about the overall properties that determine its redox activity [1, 2]. *Pseudomonas aeruginosa* cytochrome c_{551} (PA) is composed of 82 amino acid residues and possesses a unique long polypeptide loop formed from the residues at positions 50 – 68, which acts as a "lid" for the heme active site [3] (Figure 1A). Since this loop lies in close proximity to the heme, its structure and orientation, with respect to the heme, are thought to play important roles in stabilization of the heme active site structure and in determination of the heme environment. Studies on PA and its mutants as well as homologous proteins such as *Hydrogenobacter thermophilus* cytochrome c_{552} [4] revealed that the structure of this loop is highly relevant as to functional regulation of the proteins [5-7].

The structure of the loop is stabilized through a variety of non-covalent bond interactions [3]. According to the X-ray crystallographic structure of PA [3], Ser52 in the loop forms unique hydrogen bonds with the axial Met61 and the heme 13-propionate side chain, i.e., Ser52 amide NH is hydrogen bonded to axial Met61 carbonyl CO, Met61 amide NH to Ser52 carbonyl CO, and Ser52 side chain OH to the heme 13-propionate side chain (Figure 1B). Through these hydrogen bonds, Ser52 contributes significantly to determination and stabilization of the structure of the functionally relevant loop.

One of the functional characteristics of PA is that its redox potential (E_m) exhibits a large pH-dependent change, i.e., ~60 mV, due to deprotonation/protonation of the heme 17-propionic acid/propionate side chain with a pK_a value of 6.1 ± 0.2 [8-11] (Figure 1C). In general, the heme propionate side chain buried in the protein matrix of cyt *c* is hydrogen-bonded to the positively charged amino acid side chain of a Lys or Arg residue to lower its pK_a value in order to maintain a constant E_m value throughout the physiological pH range [8]. Although the X-ray structure of PA indicated that the buried heme 17-propionic acid side chain forms an ion-pair with the guanidyl group of the Arg47 side chain and a hydrogen bond with the Try56 indole NH proton [3], the pK_a

value determined for the heme 17-propionic acid side chain in the oxidized form of PA indicated that the electrostatic interaction between the heme 17-propionate and Arg47 side chains is rather weak, if any [11]. Since the heme 17-propionic acid side chain is buried under the loop (Figure 1A), the structure and orientation, with respect to the heme, of the loop is thought to be important for regulation of the environment of the heme 17-propionic acid side chain.

In this study, we determined the influence of the Ser52 mutation on the structure of the loop, the environments of the heme and the heme 17-propionic acid side chain, the stability of the coordination bond between heme Fe and Met61 in the oxidized protein (Fe^{3+}-S bond), and the E_m value through characterization of the S52N and S52G mutants in order to gain a deeper understanding as to how the structural properties of the loop are related to the functional regulation of the protein. The unique dual hydrogen bond between the residue at position 52 and Met61 is expected to be independent of the mutations. The Asn52 side chain in the S52N mutant possibly acts as a hydrogen bond donor for the heme 13-propionate side chain, as the Ser52 one in the wild-type protein does, whereas the hydrogen bond between the residue at position 52 and the heme 13-propionate side chain is completely eliminated by the S52G mutation. The study demonstrated that the functional properties of the protein were essentially unaffected by the S52N mutation, whereas the E_m value of the protein was lowered by as much as ~20 mV under acidic pH conditions due to the S52G mutation. The similarity in the E_m value between the wild-type protein and the S52N mutant indicated that the structure of the loop was hardly affected by the mutation, and hence that Asn52 in the mutant plays a similar pivotal role in the formation of the unique hydrogen bond network with the axial Met61 and the heme 13-propionate side chain that stabilizes the structure of the loop as Ser52 in the wild-type protein does. On the other hand, the effect of the S52G mutation on the E_m value could be due to a structural change of the loop due to the lack of the hydrogen bond between the Gly52 and heme 13-propionate side chains in the mutant. The negative shift of the E_m value and a decrease in the pK_a value of the heme 17-propionic acid side chain, together with smaller pH-dependent changes of the E_m value and heme peripheral methyl proton NMR shifts, are all consistent with an increase in the polarity of the heme environment in the S52G mutant.

2. Experimental

2.1. Protein Samples. The wild-type PA and the mutants were produced using *Escherichia coli* and purified as reported previously [12, 13]. The oxidized forms of the proteins were prepared by the addition of a 10-fold molar excess of potassium ferricyanide. For NMR samples, the proteins were concentrated to about 1 mM in an ultrafiltration cell (YM-5, Amicon), and then 10 % ^2H_2O was added to the protein solutions.

2.2. ^{1}H NMR. NMR spectra were recorded on a Bruker Avance 600 FT NMR spectrometer operating at a ^{1}H frequency of 600 MHz. Chemical shifts are given in parts per million downfield from sodium 2,2-dimethyl-2-silapentane-5-sulfonate with H_2O as an internal reference. ^{15}N/^{1}H heteronuclear single quantum coherence (HSQC) spectra were recorded using a standard pulse sequence. Spectra were zero-filled to give a final matrix of 2048×256 data points and apodized with a 90° shifted sine-bell window function in both dimensions. Both ^{1}H and ^{15}N chemical shifts were calibrated against the ^{1}H shift of sodium 2,2-dimethyl-2-silapentane-5-sulfonate [14].

2.3. Absorption Spectroscopy. Absorption spectra were recorded with a Beckman DU 640 spectrophotometer using a micro T_m analysis system and a micro T_m cell. The protein concentration was ~0.2 mM in 20 mM phosphate buffer (pH 7.0) in the presence of 2 mM potassium ferricyanide.

2.4. Cyclic Voltammetry. The procedures used for obtaining cyclic voltammograms for the proteins were essentially the same as those described previously [5, 15]. CV experiments were performed with a Potentiostat-Galvanostat PGSTAT12 (Autolab, Netherland). A glassy carbon electrode (GCE) was polished with a 0.05 μm alumina slurry and then sonicated in deionized water for 1 min. Two μl of a 1 mM protein solution was spread evenly with a microsyringe onto the surface of the GCE. Then the GCE surface was covered with a semipermeable membrane. All E_m values were referenced to a standard hydrogen electrode. The experimental error for the E_m value was ± 5 mV. The anodic to cathodic peak current ratios obtained at various potential scan rates (1 – 100 mV s^{-1}) were all ~1. Both the anodic and cathodic peak currents increased linearly as a function of the square root of the scan rate in the range up to 100 mV s^{-1}. Thus, PA and its mutants exhibited quasi-reversible redox processes.

3. Results

3.1. ^{1}H NMR spectra of PA and its Ser52 mutants

We first analyzed the effects of the Ser52 mutations on the heme electronic structure of the protein by ^{1}H NMR. The NMR spectra of the oxidized forms of PA and its mutants are compared in Figure 2. The heme electronic structures of the oxidized proteins have been shown to be sensitively manifested in paramagnetic shifts of the heme peripheral side chain proton signals [16-19]. The spectral patterns observed for all the proteins were similar to each other, indicating that the structural properties of the heme active site of PA were hardly affected by the mutations. The similarity in the structure among the proteins was also supported by the results of structural characterization using ^{1}H-^{15}N HSQC spectra sensitive to protein folding (Supporting information). The HSQC cross-peaks of the S52G mutant nearly completely overlapped with the corresponding ones of the wild-type protein, except those due to residues near the substituted residue (Figure 3), indicating that the protein folding was not significantly affected by the mutation. Thus, these NMR results confirmed that the structural alteration induced by the mutations was localized only in the loop.

We then investigated the pH dependence of ^{1}H NMR spectra of the oxidized proteins in order to determine the effects of the Ser52 mutations on the pK_a value of the buried heme 17-propionic acid side chain, which has been shown to significantly affect the E_m value of the protein (Supporting information). The pH-profiles of the heme methyl proton shifts for the mutants, together with those of PA, are compared in Figure 4. The pK_a value of the heme 17-propionic acid side chain in the S52N mutant was essentially equal to that of the wild-type protein, and that of the S52G mutant was lower by ~0.5 (Table 1). The change in the pK_a value due to the S52G mutation is likely to be due to an alteration in the environment of the heme 17-propionic acid side chain caused by the mutation. Furthermore, upon deprotonation/protonation of the heme 17-propionic acid/propionate side chain, the heme 18-methyl proton NMR signals of the wild-type PA, and the S52N and S52G mutants exhibited shift changes of 2.8, 2.8, and 0.9 ppm, respectively. The smaller pH-dependent shift change of the heme 18-methyl proton signal of the S52G mutant, compared with those of the other two proteins, also supported that the environment of the heme 17-propionic acid side chain of the protein was affected by the S52G mutation.

3.2. Thermostability of the Fe^{3+}-S coordination bonds in the Ser52 mutants.

We also examined the thermostability of the Fe^{3+}-S coordination bond in the oxidized forms of the Ser52 mutants through analysis of the temperature dependence of the 695-nm absorption characteristic of the bond (Figure 5 and Supporting information). The disruption of the Fe^{3+}-S bond upon thermal denaturation of a protein was manifested in the disappearance of the absorbance with increasing temperature. In the case of the S52N mutant, a disruption temperature of 81 ºC for the Fe^{3+}-S bond ($T_{m(Fe\text{-}S)}$) was obtained as the midpoint in the plots of the normalized absorbance against temperature, which is almost the same as that of PA (Table 1). The similarity in the $T_{m(Fe\text{-}S)}$ value between PA and the S52N mutant supported that the Asn52 side chain in the mutant plays a similar role to the Ser52 one in the wild-type protein in stabilization of the structure of the loop. On the other hand, the $T_{m(Fe\text{-}S)}$ value of the S52G mutant was lower by ~6 ºC relative to that of the wild-type protein. Since the Gly52 side chain cannot be involved in the formation of a hydrogen bond, the decrease in the thermostability of the Fe^{3+}-S bond in the S52G mutant relative to that in the wild-type protein could be due to the absence of the hydrogen bond between the G52 and heme 13-propionate side chains in the mutant.

3.3. E_m values of the Ser52 mutants.

We next measured the E_m values of the S52N and S52G mutants at various pHs, and the obtained values, together with those of the wild-type protein, for comparison, are plotted against pH in Figure 6. The pH profiles of the E_m values of PA and the S52N mutant were quite similar in pattern to each other, the exception being the difference of ~5 mV in its magnitude throughout the pH range examined, i.e., pH ~4.5 - ~9.0. On the other hand, the pH profile of the E_m values of the

S52G mutant was different from those of the others, in terms of the magnitude of the pH-dependent E_m change ($\Delta E_{m(\mathrm{pH})}$) throughout the pH range examined, i.e., the $\Delta E_{m(\mathrm{pH})}$ values of the S52G mutant and PA (or the S52N mutant) were ~40 and ~60 mV, respectively, although the E_m values of the three proteins at pH 9 were similar to each other (Table 1).

As has been demonstrated previously [11], the pK_a value of the heme 17-propionic acid side chain is reflected in the pH-profile of the E_m value. The fitting of the plots in Figure 6 to the Nernst equation yielded pK_a values of 6.0 ± 0.2 and 7.1 ± 0.2 for the oxidized and reduced forms (p$K_{\mathrm{a(ox)}}$ and p$K_{\mathrm{a(red)}}$) of the S52N mutant, respectively, and p$K_{\mathrm{a(ox)}}$ and p$K_{\mathrm{a(red)}}$ values of 5.2 ± 0.2 and 6.0 ± 0.2, respectively, were yielded for the S52G mutant. The plot for the S52N mutant at pH <4.5 deviated from the Nernst equation, possibly reflecting the protonation of the heme 13-propionate side chain. The obtained p$K_{\mathrm{a(ox)}}$ values of the proteins were similar to the pK_a values of the heme 17-propionic acid side-chains in the corresponding proteins.

4. Discussion

4.1. The effects of the Ser52 mutations on the pK_a value of the heme 17-propionic acid side chain

pK_a values of 6.0 ± 0.2 and 5.2 ± 0.2 were obtained for the oxidized forms of the S52N and S52G mutants, respectively (Table 1), and the value of 6.1 ± 0.2 has been reported for the wild-type protein [11]. The pK_a values of heme propionic acid side chains have been shown to be sensitive to their environment. In fact, the pK_a value of the solvent-exposed heme 13-propionic acid side chain was reported to be ~3.5 [10], and, on the other hand, the decrease in the acidity of the heme 17-propionic acid side chain in a hydrophobic environment was manifested in its larger pK_a value, i.e., 6.1 ± 0.2.

Ser52 in the wild-type protein is located in close proximity to the heme 17-propionic acid side chain, in spite of no direct interaction between them, and the heme 17-propionic acid side chain is buried under the loop [3] (Figure 1A). The similarity in the pK_a value of the heme 17-propionic acid side chain between the wild-type protein and the S52N mutant indicated that these two proteins are similar to each other in terms of the environment of the heme 17-propionic acid side chain, and hence the structure of the loop. This finding suggested that the Asn52 side chain in the mutant forms a hydrogen bond with the heme 13-propionate side chain, as the Ser52 one in the wild-type protein does.

On the other hand, the ~0.5 decrease in the pK_a value due to the S52G mutation is likely to be due to an increase in the polarity of the environment of the heme 17-propionic acid side chain due to a structural alteration of the loop induced by the elimination of the hydrogen bond between the residue at position 52 and the heme 13-propionic acid side chain in the mutant. Therefore, the hydrogen bond between the residue at position 52 and the heme 13-propionic acid side chain appears to be crucial for regulation of the environment of the heme 17-propionic acid side chain.

4.2. The effects of the Ser52 mutations on the stability of the Fe^{3+}-S coordination bond

We previously showed that the stability of the Fe^{3+}-S coordination bond, as reflected in the $T_{m(Fe\text{-}S)}$ value, correlates with that of the hydrophobic core near the heme in the protein [11, 20]. The $T_{m(Fe\text{-}S)}$ values of the S52N and S52G mutants were determined to be 81 and 72 ºC, respectively, and were compared with that of the wild-type protein, i.e., 78 ºC [11, 20, 21]. The similarity in the $T_{m(Fe\text{-}S)}$ value between the S52N mutant and the wild-type protein demonstrated that the stabilities of the Fe^{3+}-S bond, and hence the hydrophobic environments of the heme active site, in the two proteins are almost the same as each other. Consequently, the Asn52 side chain in the mutant was found to form a hydrogen bond with the heme 13-propionate side chain, as the Ser52 one in the wild-type protein does. Thus, the formation of the hydrogen bond between the Asn52 and heme 13-propionic acid side chains in the mutant was also confirmed through analysis of the thermostability of the Fe^{3+}-S bond. On the other hand, the lower $T_{m(Fe\text{-}S)}$ value of the S52G mutant indicated that the hydrophobic environment of the heme active site in the S52G mutant was considerably deteriorated in the absence of the hydrogen bond between the Gly52 and heme 13-propionate side chains in the mutant. Thus, the hydrogen bond between the residue at position 52 and the heme 13-propionate side chain plays an important role in stabilization of the hydrophobic environment of the heme active site.

4. 3. The effects of the Ser52 mutations on the E_m value

The pH profile of the E_m values of the S52N mutant was similar to that of the wild-type protein throughout the pH range examined. These results also supported that the structure of the loop was hardly affected by the S52N mutation. Consequently, based on the E_m, pK_a, and $T_{m(Fe\text{-}S)}$ values determined for the S52N mutant, it is concluded that the Asn52 side chain in the mutant forms a hydrogen bond with the heme 13-propionate side chain, as the Ser52 one in the wild-type protein does.

On the other hand, the pH profile of the E_m values of the S52G mutant was different from those of the others in terms of the $\Delta E_{m(pH)}$ value, i.e., the values of the S52G mutant and PA (or the S52N mutant) were ~40 and ~60 mV, respectively (Figure 6). As has been described previously [10, 11], the pH profile of the E_m values of a protein can be interpreted in terms of the deprotonation/protonation of the buried heme 17-propionic acid/propionate side chain. Since the E_m value of a protein is related to the difference in the thermodynamic stability between the two redox forms, the negative-shift of the E_m value with increasing pH is attributed to the stabilization of the cationic ferriheme in the oxidized protein, relative to the neutral ferroheme in the reduced one, in the hydrophobic environment of the heme active site through partial neutralization of its positive charge by the heme 17-propionate side chain [11]. According to the Nernst equation, the $\Delta E_{m(pH)}$ value should be ~60 mV, as observed for PA, the S52N mutant, and previously studied PA mutants [6, 11, 21]. The smaller $\Delta E_{m(pH)}$ value observed for the S52G mutant would be interpreted in terms of an increase in the polarity of the environment of the heme 17-propionic acid side chain in the mutant. The negative-shift of the E_m value by ~20 mV at acidic pH, due to the S52G mutation, also supported an increase in the polarity of the heme active site due to the mutation, because the hydrophobic environment of the heme is essential for a positive and high E_m value [1, 2]. The increase in the polarity of the environment of the heme 17-propionic acid side chain partially allows cations or solvent molecules to surround the negative charge emerging upon deprotonation of the side chain to stabilize its charge. Such electrostatic interactions would result in a decrease in the partial neutralization of the cationic ferriheme in the oxidized protein, leading to a decrease in the stabilization of the oxidized protein. As a result, the $\Delta E_{m(pH)}$ value of the S52G mutant was smaller than those of the other two proteins. Thus, the $\Delta E_{m(\mathrm{pH})}$ value was affected by the environment of the heme 17-propionic acid side chain. The present study demonstrated that the environment of the heme 17-propionic acid side chain plays crucial roles in determination of not only the pH-profile of the E_{m} value, but also that of the $\Delta E_{m(\mathrm{pH})}$ value.

4. 4. The environment of the heme 17-propionic acid side chain in the S52G mutant

As described above, the S52G mutant was different from the other two proteins in various respects. The observed differences could be attributed primarily to the lack of the hydrogen bond between the Gly52 and heme 13-propionate side chains in the mutant. The ~20 mV negative-shift of the E_{m} value, the ~0.5 decrease in the pK_{a} value of the heme 17-propionic acid side chain, and the ~6-degree lowering of the $T_{\mathrm{m(Fe\text{-}S)}}$ value are all consistent with an increase in the polarity of the heme active site due to the mutation. Consequently, the smaller pH-dependent shift changes of the heme methyl proton signals of the S52G mutant could also be attributed to the increase in the polarity of the heme active site in the mutant. The pH-dependent shift changes of the heme methyl proton signals upon deprotonation/protonation of the buried heme 17-propionic acid/propionate side chain are thought to be due to through-space and –bond inductive effects of the appearance/disappearance of the negative charge on the heme π-system. Such inductive effects of the heme 17-propionic acid side chain of the heme electronic structure could become smaller with increasing the polarity of the heme side chain.

5. Conclusion

The structure of the loop in close proximity to the heme in the protein has been shown to be affected by the elimination of the hydrogen bond between the Ser52 and heme 13-propionate side chains by the S52G mutation. The structural change of the loop induced by the mutation resulted in a slight increase in the polarity of the heme environment, which was sharply manifested in an alteration of the pH-profile of the E_m value. Thus, the present study demonstrated that the redox function of the protein can be finely tuned through the structural properties of the polypeptide loop near the heme. This finding provides novel insights as to tuning of the redox function of the protein through protein engineering.

6. Abbreviations

cyt *c*, cytochrome *c*

PA, *Pseudomonas aeruginosa* cytochrome c_{551}

E_m, redox potential

Fe^{3+}-S bond, the coordination bond between heme Fe and Met61 in the oxidized protein

HSQC, heteronuclear single quantum coherence

GCE, glassy carbon electrode

$T_{m(Fe\text{-}S)}$, the disruption temperature of the Fe^{3+}-S bond

$\Delta E_{m(pH)}$, the magnitude of the pH-dependent E_m change

$pK_{a(ox)}$, the pK_a value of the heme 17-propionic acid side chain for the oxidized protein

$pK_{a(red)}$, the pK_a value of the heme 17-propionic acid side chain for the reduced protein.

Acknowledgements

We are indebted to Dr. Shin Kawano for the assistance with the initial experiments. This work was supported by Grants-in-Aid for Scientific Research on Innovative Areas (No. 23108703, "π-Space", and 23655151) from the Ministry of Education, Culture, Sports, Science and Technology, Japan, the Yazaki Memorial Foundation for Science and Technology, and the NOVARTIS Foundation (Japan) for the Promotion of Science. The NMR spectra were recorded on Bruker AVANCE-600 spectrometers at the Chemical Analysis Center, University of Tsukuba.

Supporting Information

Superpositioning of $^{15}N/^{1}H$ HSQC spectra of the oxidized forms of ^{15}N-uniformly labeled wild-type PA and the S52G mutant in 90 % H_2O/10 % $^{2}H_2O$, pH 6.0, at 23 ºC, 600 MHz ^{1}H NMR spectra of the oxidized forms of PA and, the S52N and S52G mutants in 90% H_2O/10% $^{2}H_2O$ at various pHs and 25 ºC, temperature dependence of absorption spectra (600–800 nm) of the S52N and S52G mutants.

References

1. G.R. Moore, G.W. Pettigrew, Cytochromes *c*: Evolutionary, structural, and physicochemical aspects, Springer-Verlag, Berlin, 1991.
2. R.A. Scott, A.G. Mauk, Cytochrome *c*: A multidisciplinary approach. University Science Books, Sausalito, 1996.
3. Y. Matsuura, T. Takano, R.E. Dickerson, J. Mol. Biol. 156 (1982) 389-409.
4. Y. Sanbongi, M. Ishii, Y. Igarashi, T. Kodama, J. Bacteriol. 171 (1989) 65-69.
5. S.J. Takayama, Y. Takahashi, S. Mikami, K. Irie, K. Kawano, Y. Yamamoto, H. Hemmi, R. Kitahara, S. Yokoyama, K. Akasaka, Biochemistry 46 (2007) 9215-9224.
6. S. Mikami, H. Tai, Y. Yamamoto, Biochemistry 49 (2010) 42-48.
7. H. Tai, K. Irie, S. Mikami, Y. Yamamoto, Biochemistry 50 (2011) 3161-3169.
8. G.R. Moore, G.W. Pettigrew, R.C. Pitt, R.J.P. Williams, Biochim. Biophys. Acta 590 (1980) 261- 271.
9. G.R. Moore, FEBS Lett. 161 (1983) 171-175.
10. F.A. Leitch, G.R. Moore, G.W. Pettigrew, Biochemistry 23 (1984) 1831-1838.
11. S.J. Takayama, S. Mikami, N. Terui, H. Mita, J. Hasegawa, Y. Sambongi, Y. Yamamoto, Biochemistry 44 (2005) 5488-5494.
12. J. Hasegawa, H. Shimahara, M. Mizutani, S. Uchiyama, H. Arai, M. Ishii, Y. Kobayashi, S.J. Ferguson, Y. Sambongi, Y. Igarashi, J. Biol. Chem. 274 (1999) 37533-37537.
13. J. Hasegawa, S. Uchiyama, Y. Tanimoto, M. Mizutani, Y. Kobayashi, Y. Sambongi, Y. Igarashi, J. Biol. Chem. 275 (2000) 37824-37828.
14. D.S. Wishart, C.G. Bigam, J. Yao, F. Abildgaard, H.J. Dyson, E. Oldfield, J.L. Markley, B.D. Sykes, J. Biomol. NMR 6 (1995) 135–140.
15. E. Lojou, P. Bianco, J. Electroanal. Chem. 485 (2000) 71-80.
16. G.N. La Mar, J.D. Satterlee, J.S. de Ropp, Nuclear magnetic resonance of hemoproteins, in The Porphyrin Handbook (K. Kadish, K.M. Smith, R. Guilard, eds.), pp 185-298, Academic Press, New York, 2000.

17. I. Bertini, C. Luchinat, NMR of Paramagnetic Molecules in Biological Systems, pp 19-46, The Benjamin/Cummings Publishing Company, Menlo Park, California, 1986.
18. Y. Yamamoto, Annu. Rep. NMR Spectrosc. 36 (1998) 1-77
19. Y. Yamamoto, N. Terui, N. Tachiiri, K. Minakawa, H. Matsuo, T. Kameda, J. Hasegawa, Y. Sambongi, S. Uchiyama, Y. Kobayashi, Y. Igarashi, J. Am. Chem. Soc. 125 (2002) 13650-13651.
20. Y. Takahashi, H. Sasaki, S.J. Takayama, S. Mikami, S. Kawano, H. Mita, Y. Yamamoto, Biochemistry 45 (2006) 11005-11011.
21. S.J. Takayama, K. Irie, H. Tai, T. Kawahara, S. Hirota, T. Takabe, L.A. Alcaraz, A. Donaire, Y. Yamamoto, J. Biol. Inorg. Chem. 14 (2009) 821-828.

Figure captions

Figure 1. (A) Schematic representation of the structure of *Pseudomonas aeruginosa* cytochrome c_{551} (PA), and the locations of the Ser52 and axial Met61 residues, and the loop composed of the residues at positions 50 through 68 [3]. The polypeptide chain is illustrated as a ribbon model and the heme is drawn as a ball-and-stick model. (B) Schematic representation of the unique hydrogen bond network among Ser52, Met61, and the heme 13-propionate side chain of PA. Ser52 amide NH is hydrogen bonded to axial Met61 carbonyl CO, Met61 amide NH to Ser52 carbonyl CO, and Ser52 side chain OH to the heme 13-propionate side chain. (C) pH-profile of the redox potential (E_m) of PA at 25 °C. The pH-dependent E_m change of ~60 mV is due to deprotonation/protonation of the heme 17-propionic acid/propionate side chain with a pK_a value of 6.1 ± 0.2 [8-11].

Figure 2. 600 MHz ^{1}H NMR spectra of the oxidized forms of PA (A), and the S52N (B) and S52G (C) mutants in a 90% H_2O/10% ^2H_2O mixture at pH 7.0 and 25 ºC. The assignments of the heme methyl and resolved axial Met61 side chain proton signals are given with the spectra, and the corresponding signals in the spectra are connected by dotted lines.

Figure 3. Plots of the shifts (ppm) for the main chain amide ^{1}H (bottom) and ^{15}N (top) NMR signals of the S52G mutant relative to those of the corresponding ones of the wild-type PA in 90% H_2O/10% ^2H_2O, pH 6.0, at 23 °C ($\Delta\delta_{S52G\text{-}PA}$) against the amino acid residue number. The effects of the S52G mutation on the main chain amide ^{1}H and ^{15}N signals are mostly localized in the loop

composed of the residues at positions 50 – 68. The amino acid sequence of the loop is indicated between the plots of the ^{1}H and ^{15}N shifts.

Figure 4. pH-dependence of the chemical shifts of heme methyl proton signals of the oxidized forms of PA (A), and the S52N (B) and S52G (C) mutants in 90% H_2O/10% $^{2}H_2O$ at 25 °C. The pK_a value of the heme 17-propionic acid side chain is reflected in the pH-dependence shifts.

Figure 5. Plots of the normalized 695-nm absorption of the oxidized forms of the wild-type PA (○) [11], and the S52N (▲) and S52G (●) mutants at pH 7.00 against temperature. The absorption was normalized in such a way that the values at 25 ºC equal 1.0. The disruption temperatures of the Fe^{3+}-S bond ($T_{m(Fe\text{-}S)}$) in the proteins are taken as the midpoints in the plots.

Figure 6. pH-profiles of the E_m values of the S52N (▲) and S52G (●) mutants, together with that of the wild-type PA (○) [8-11], for comparison, at 25 °C. The solid curves are theoretical curves drawn using the pH-dependent form of the Nernst equation, $E_m = E_{mH} - 0.06 \times \log\{(K_{ox} + [H^+])/(K_{red} + [H^+])\}$, where the E_{mH} is the E_m of the fully protonated form, and K_{ox} and K_{red} are the equilibrium constants for the ionization in the oxidized and reduced proteins, respectively.

Table 1. Heme methyl and selected axial Met61 proton NMR shifts, pK_a values, E_m values, and disruption temperatures of the Fe^{3+}-S bonds of wild-type PA and S52N and S52G mutants.

	Heme methyl[a] (ppm)				Axial Met61[a] (ppm)			NMR	CV		E_m[d]	$T_{m(Fe\text{-}S)}$[e]
Protein	12-Me	2-Me	18-Me	7-Me	$C_\gamma H$	$C_\varepsilon H_3$	$C_\gamma H'$	pK_a[b]	pK_{ox}[c]	pK_{red}[c]	(mV)	(°C)
PA	31.89	24.72	17.84	13.30	-8.43	-16.73	-40.41	6.1	5.9	7.0	260	78
S52N	32.01	24.71	17.88	13.21	-8.43	-16.85	40.76	6.0	6.0	7.1	267	81
S52G	31.58	24.17	17.89	13.85	-9.26	-16.97	-38.94	5.4	5.2	6.0	256	72

[a] Shifts at 25 ºC.

[b] The value was obtained from the pH-dependent shifts of heme methyl proton signals of the oxidized form of the protein. The experimental error was ± 0.2.

[c] pK_{ox} and pK_{red} represent the pK_a values of the oxidized and reduced forms of the protein, respectively, determined on fitting of the pH profile of the E_m value to the Nernst equation. The experimental error was ± 0.2.

[d] Determined at pH 5.0 and 25 ºC. The experimental error determined from deviation of two or more experiments was ±5 mV.

[e] Disruption temperature of the Fe^{3+}-S coordination bond of the oxidized protein at pH 7.0, determined from the temperature dependence of the 695-nm absorption band characteristic of the bond.

Figure 1

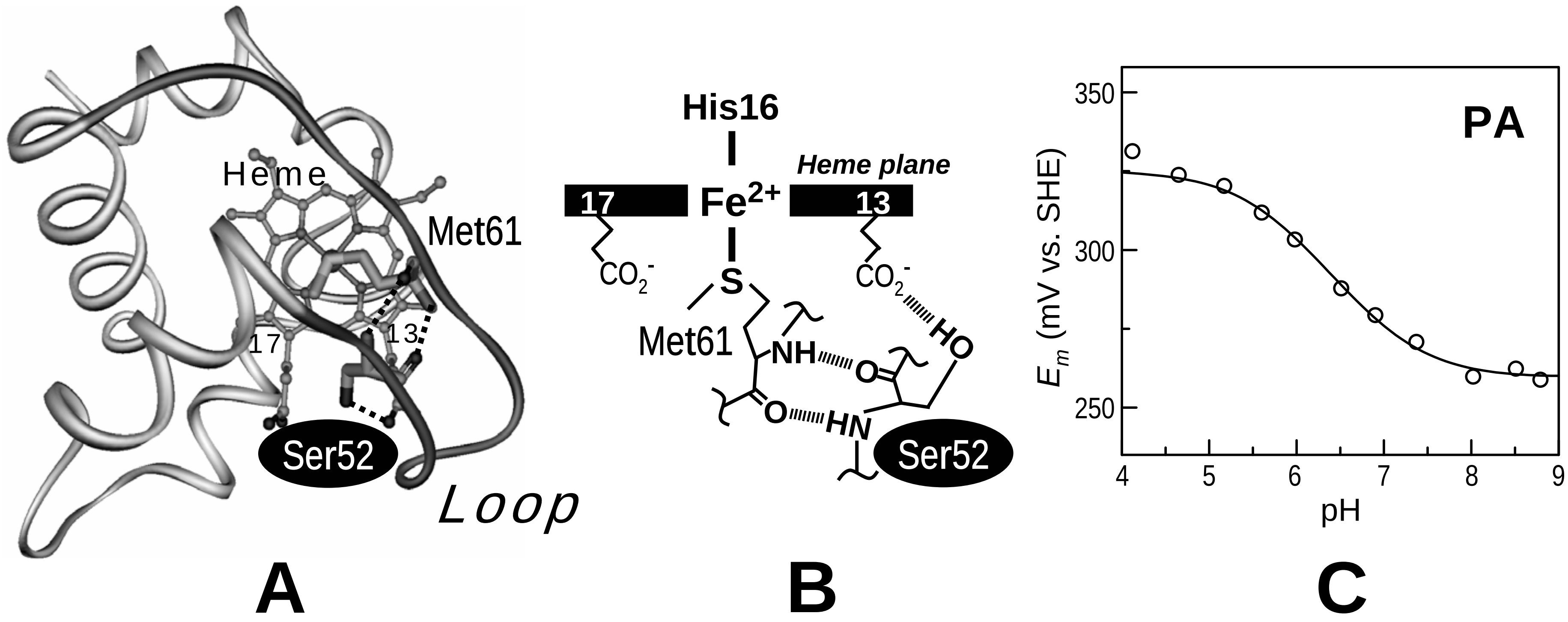

Heme
Met61
17
13
Ser52
Loop
His16
Heme plane
17
Fe2+
13
CO2-
CO2-
S
Met61
NH
O
HO
O
HN
Ser52
PA
Em (mV vs. SHE)
350
300
250
4
5
6
7
8
9
pH
A
B
C

Figure 2

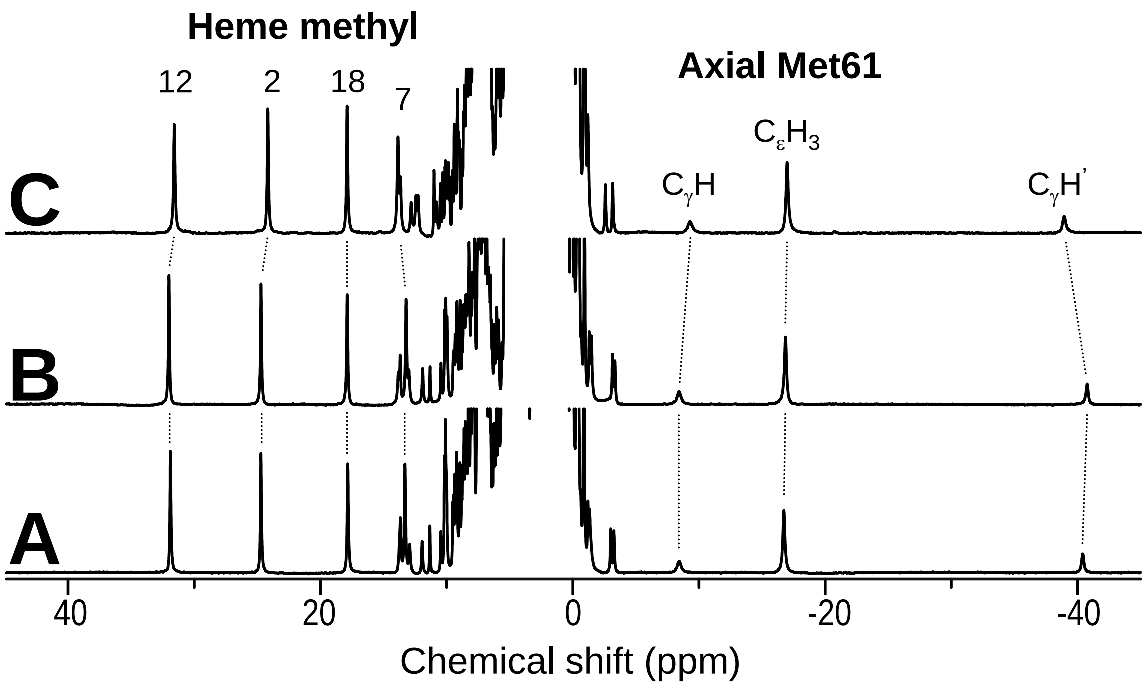
Heme methyl
12
2
18
7
Axial Met61
CεH3
CγH
CγH'
C
B
A
40
20
0
-20
-40
Chemical shift (ppm)

Figure 3

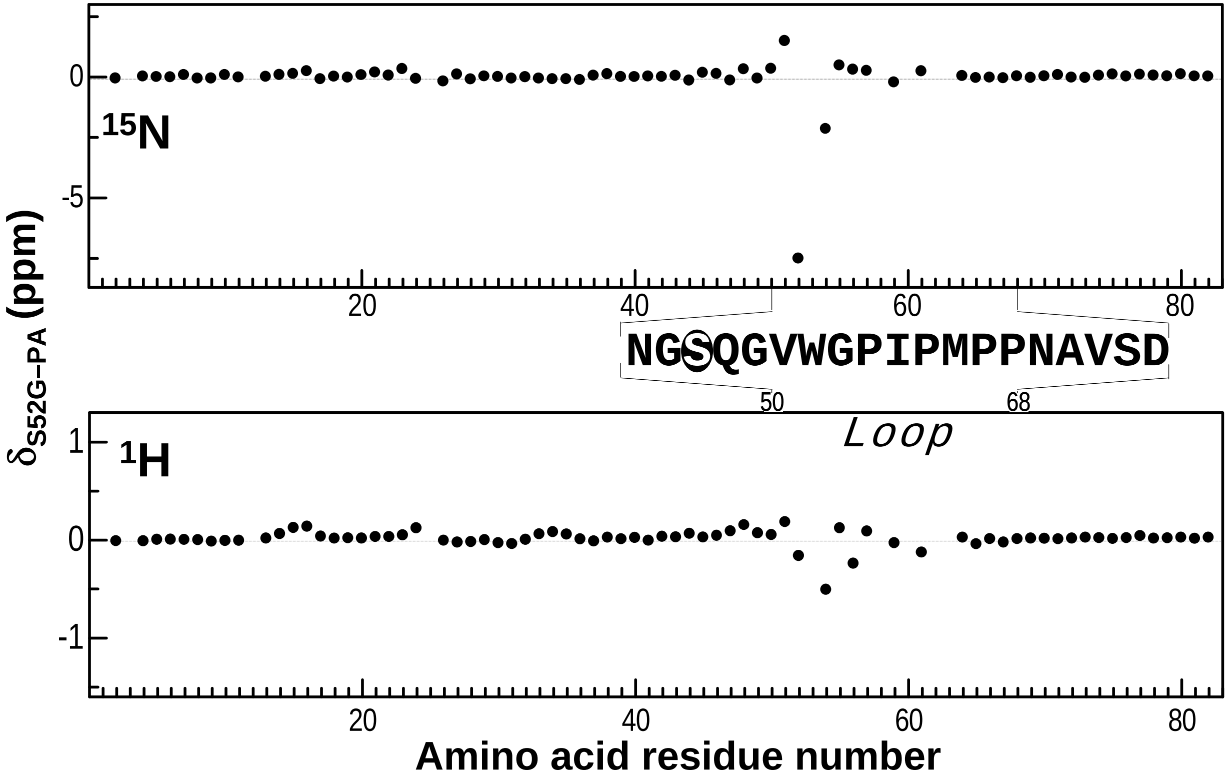

0
-5
^{15}N
20
40
60
80
$\delta_{S52G-PA}$ (ppm)
NGSQGVWGPIPMPPNAVSD
50
68
Loop
1
0
-1
^{1}H
20
40
60
80
Amino acid residue number

Figure 4

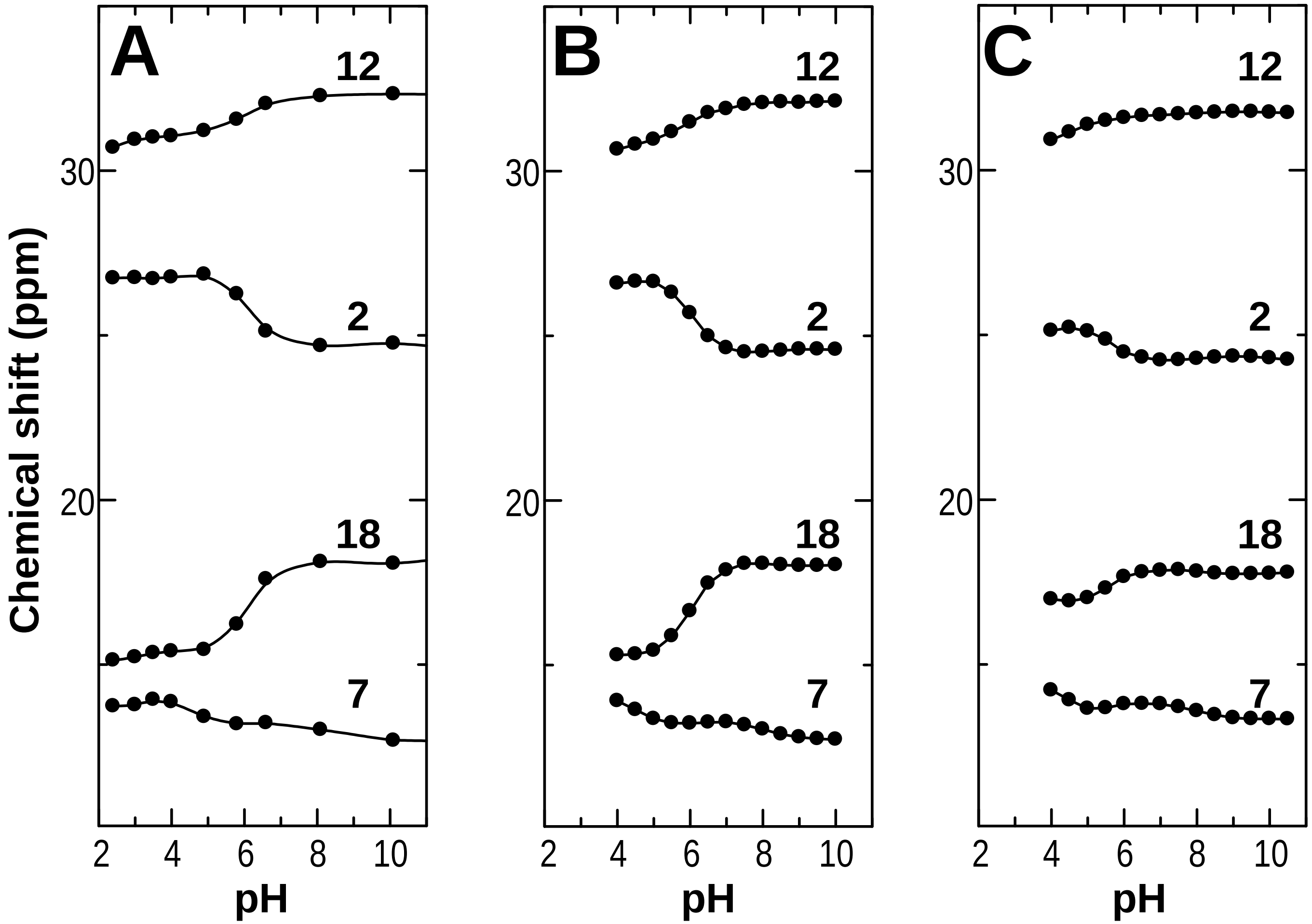

Figure 5

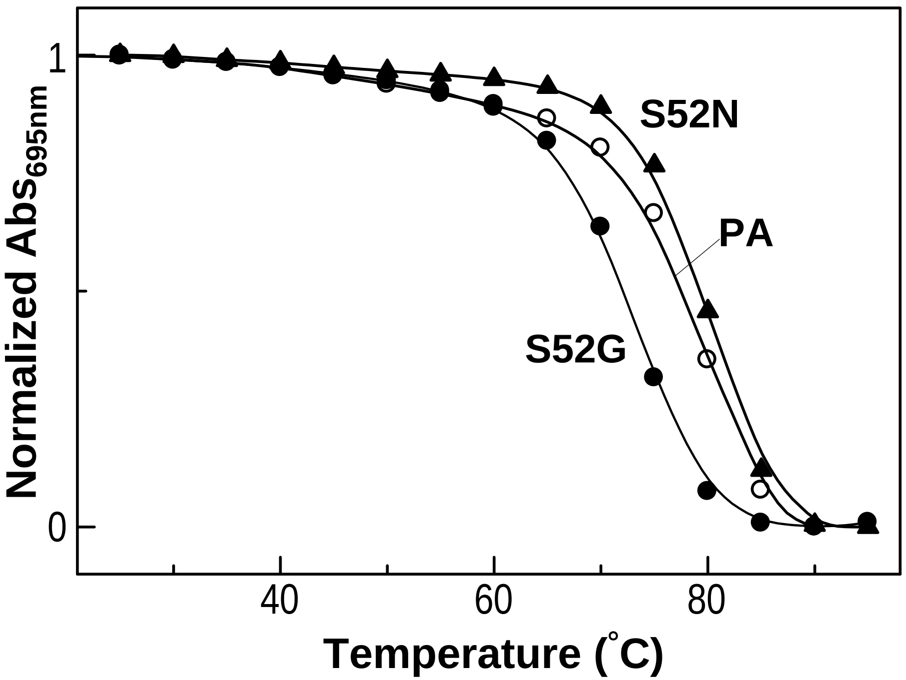

Figure 6